

INTRODUCTION

Exploring the structure, stability and bonding associated with ionic materials has a long history^{1,2}. A popular theme has been to match chemical and physical properties via electrostatic potentials. For example, at an undergraduate level it is common to model lattice energies of bulk materials using Born-Mayer-like potential functions³. In these, the principal bonding contribution is provided by monopole-monopole coulombic interactions, although Van der Waals and polarization contributions must also be included for completeness⁴. Madden and Wilson⁵ have indeed emphasized polarization effects in rationalizing the structure and bonding associated within the loose terminology of ionic materials. This is addressed later in the discussion section.

Recently, there has been a renewed and related theoretical interest targeting nanostructures of these materials, including NaCl^{6,7}, MgO⁸, LiF⁷ and organic salts⁹, with the most common approach stemming from Density Functional Theory (DFT). Even prior to the recent surge of interest in nanoscience, there were many theoretical discussions concerning the structure and bonding occurring in alkali halide clusters. Most notably, Martin was a pioneer in this area². Recently, Maroulis¹⁰ has described how DFT calculations on NaCl can be used as a “test case” in evaluating the efficacy of quantum mechanical calculations on small NaCl clusters. We continue in this vein using both DFT and Madelung constant evaluations to explore the structure and bonding (most notably the ionic charge) on model NaCl nanotubes.

The approach that we use in this paper involves calculating the cohesive energies of NaCl nanotubes via a combination of DFT and MC(wa) determinations. We indeed recently reported a linear correlation between cohesive energies generated by DFT calculations and (MC(wa))¹¹, which is utilized throughout this paper. Furthermore, the DFT-Madelung relationship is used to

structure, which is calculated from a conditionally convergent summation, $MC(wa)$ values are determined from a finite sum over each nanotube.

DFT calculations were effected using the Gaussian 09 suite¹³ within Microsoft Windows and Macintosh OS X platforms. Energy minimizations were achieved using a 6-311G(d) basis set plus a B3LYP functional. In all DFT geometry optimizations, a subsequent frequency calculation was performed to confirm that a true minimum, rather than a saddle point, was located. Cohesive energies in this paper are given in eV. Other energies and charges are reported in eV or atomic units as specified in the Tables. The formalism used to describe the nanotubes is described below, and single ion MC values are shown in Figure 1.

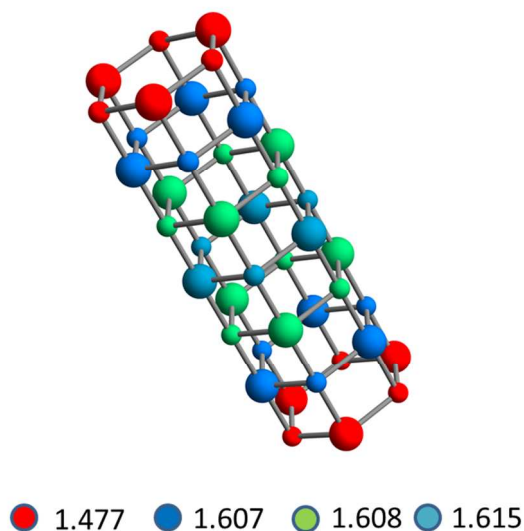


Figure 1. Madelung Constants for a 7L6 NaCl nanotube: Note that anions and cations in each layer have the same values. $MC(wa)$ is determined from the population distributions of the individual Madelung Constants. For this nanotube $MC(wa) = 1.572$ (see also Table 2). The least stable ions are situated at tube ends ($MC = 1.477$) and the most stable are located in the central layer ($MC = 1.615$).

In this paper, each nanotube is identified by the geometry of the polygon base and the number of layers of the stacked polygons. For example, a nanotube composed of a planar hexagonal base and 7 repeat units (see Figure 1), is described as a 7L6 tube which explicitly defines seven layers of six ions assembled from a hexagonal base. Collectively, nanotubes are referred to using the base polygon, and so the 7L6 structure is a member of the L6 family of nanotubes. Note that this ideal symmetry was used as an initial guess input for the DFT calculation. Optimized geometries are slightly distorted as we have reported previously for MgO nanotubes.¹¹ Examples are shown in Fig 2 for three L6 nanotubes. In each case the distortion is small, where the average bond length decreased from 2.8 Å (unoptimized geometry) to 2.7 Å (also see Table 2). Note that the dimensions are not to scale in the Figure.

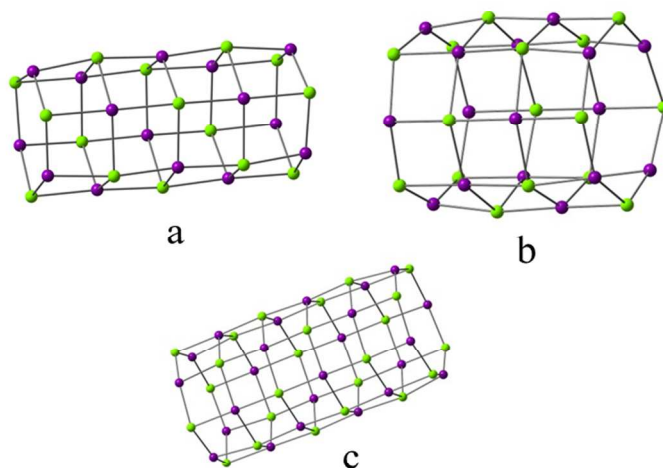
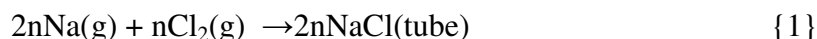


Fig 2. Examples of slight distortions for optimized NaCl nanotubes: a) 5L6. b) 4L6 . c) 6L6

The cohesive energy E_{coh} was determined from the net chemical reaction to form the nanotube.¹⁴



n is the number of ion pairs in the nanotube, and $2nE_{\text{coh}}$ is the energy change associated with the reaction. Thus;

$$E_{\text{coh}} = 1/n[E(\text{tube}) - nE_0(\text{Na}) - n/2 E_0(\text{Cl}_2)] \quad \{2\}$$

$E(\text{tube})$ is the total energy of the nanotube determined by DFT (see column 2 in Tables 1-3) and $E_0(\text{Na})$ and $E_0(\text{Cl}_2)$ are the ground state electronic energies of Na and Cl_2 , serving as an arbitrary reference. Using a 6-311G(d) basis set and a B3LYP functional, the energies of gas phase Na and Cl_2 were -162.2866299 and -920.4056758 a.u. respectively. The reference energy was therefore $(-162.2866299 + 1/2 (-920.405678)) = -622.4894678$ a.u. However, for percentage ionicity calculations, we used the combined energies of gas phase Na^+ and Cl^- ions (-162.0874615 a.u. and -460.3007103 a.u. respectively) to provide a reference energy of -622.3881718 a.u. Data analyses and fits were conducted using the Origin 7 suite (Origin Lab, Northampton MA). Graphical depictions of the nanotubes were generated using Chemcraft and Mathematica Software. Average near-neighbor distances in optimized structures were determined using the distance matrix produced by the Gaussian 09 software. Ionic charges were determined from the slopes of the E_{coh} vs. MC(wa) plots as we have described for MgO nanotubes in a previous publication¹¹. It is important to note that no specific charges or distances are assumed in the Madelung Constant derivation. Although the charges and distances are for convenience set to

unity in the computer code, they can be any value as ultimately they cancel because the dimensionless MC is a ratio of the average interionic Coulombic energy in the tube of interest divided by the Coulombic energy of a single ion pair having the same average charges and distances.

Coulombic attractive energies (E_{coul} : equation {3}) were computed using average near-neighbor distances and charges determined from the E_{coh} vs. MC(wa) plots¹¹. This is described below (see also equation {3}). The average coordination number (ACN, vide infra, discussion of Figure 4) was calculated by considering that in any nanotube, the ions in the two end layers have a coordination number of 3, while all ions in interior layers have a coordination number of 4. So, $ACN = [(2 \times 3) + 4(L-2)]/L$, where L is the number of layers.

RESULTS AND DISCUSSION

In this paper we present DFT and MC(wa) determinations for NaCl nanotubes, which are used as an archetype to convey a new method for assessing partial ionic charges associated with charge transfer (CT) effects in alkali halides and related structures. This is achieved via the linear correlation between E_{coh} and $(\text{MC}(\text{wa}))^{11}$ (see Tables 1-3 and Figure 3). Recall that the cohesive energy is relative to the energy of the ground state atoms (see equation {2} above) and will not scale linearly with the coulombic attractive energies which are by definition relative to the energies of the gas-phase ions.

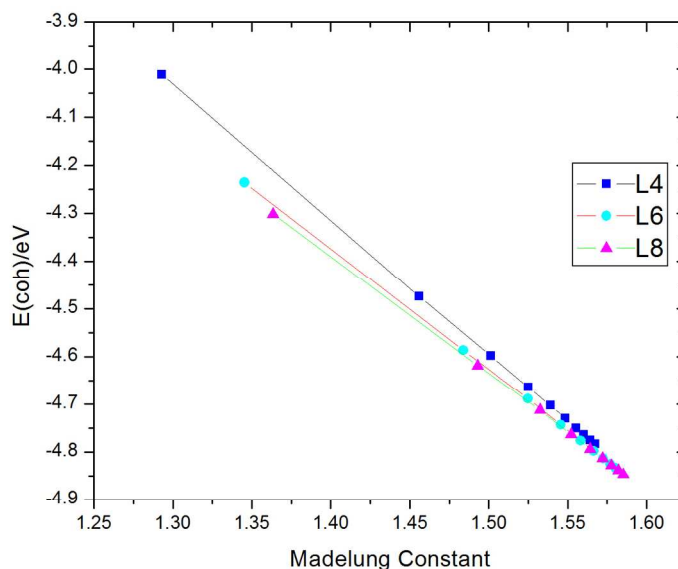


Figure 3. Linear correlation between cohesive energies and weighted-average Madelung Constants for geometry (DFT) optimized L4, L6 and L8 NaCl nanotubes (top to bottom). In each case the correlation coefficient is 1.

Table 1. Data for the L4 family of NaCl nanotubes.

tube	E(tube)/a.u.	E_{coh}/eV	$z/\text{a.u.}$	$r(\text{av})/\text{\AA}$	MC(wa) ^a	% ionic ^b	$E_{\text{coul}}/\text{eV}^c$
1L4	-1245.27375	-4.01156	0.703	2.555	1.292	53.2	-3.59711
2L4	-2490.615615	-4.474532	0.717	2.659	1.456	56.1	-4.05371
3L4	-3735.950624	-4.597897	0.722	2.693	1.501	56.8	-4.179
4L4	-4981.287051	-4.664403	0.723	2.703	1.524	57.2	-4.24304
5L4	-6226.623067	-4.703188	0.724	2.710	1.538	57.4	-4.28201
6L4	-7471.959276	-4.729482	0.724	2.714	1.548	57.6	-4.30985
7L4	-8717.2963749	-4.749993	0.725	2.716	1.555	57.7	-4.32934
8L4	-9962.632714	-4.764091	0.725	2.718	1.560	57.8	-4.34326
9L4	-11207.969050	-4.775041	0.725	2.720	1.564	57.9	-4.3544
10L4	-12453.305391	-4.783811	0.725	2.721	1.567	57.9	-4.36275

^aMC(wa) values are given to 3 decimal places. Refer to Table 1 reference 11 for more significant figs. ^b% ionic is the ratio: $100 \times E_{\text{coul}}/(E_{\text{(tube)}} - E(\text{Na}^+ + \text{Cl}^-))$. ^c See equation {3} and discussion below.

Table 2. Data for the L6 family of NaCl nanotubes.

tube	E(tube)/a.u.	E_{coh}/eV	$z/\text{a.u.}$	$r(\text{av})/\text{\AA}$	MC(wa) ^a	% ionic ^b	$E_{\text{coul}}/\text{eV}^c$
1L6	-1867.93542	-4.236058	0.669	2.536	1.345	48.8	-3.41526
2L6	-3735.948195	-4.586881	0.684	2.651	1.483	51.3	-3.76568
3L6	-5603.950777	-4.672982	0.688	2.685	1.524	52.1	-3.86978
4L6	-7471.965523	-4.743468	0.690	2.697	1.545	52.3	-3.92311
5L6	-9339.977949	-4.776384	0.691	2.7037	1.558	52.5	-3.95612
6L6	-11207.98432	-4.798124	0.691	2.7077	1.566	52.6	-3.97643
7L6	-13075.993620	-4.813561	0.691	2.7107	1.572	52.7	-3.99167
8L6	-14944.002941	-4.825163	0.692	2.713	1.577	52.8	-4.00436
9L6	-16812.011939	-4.833861	0.692	2.714	1.580	52.9	-4.01198

^a MC(wa) values are given to 3 decimal places. Refer to Table 1 reference 11 for more significant figs. ^b See footnote b for Table 1. ^c See equation {3} and discussion below.

Table 3. Data for the L8 family of NaCl nanotubes.

tube	E(tube)/a.u.	E _{coh} /eV	z /a.u	r (av)/Å	MC(wa) ^a	% ionic ^b	E _{coul} /eV ^c
1L8	-2490.590210	-4.301703	0.657	2.531	1.363	47.4	-3.34371
2L8	-4981.273782	-4.619269	0.672	2.649	1.493	49.7	-3.66263
3L8	-7471.95167	-4.712235	0.676	2.684	1.532	50.3	-3.7583
4L8	-9962.632669	-4.764008	0.678	2.696	1.552	50.6	-3.80737
5L8	-12453.31278	-4.793864	0.679	2.703	1.564	50.8	-3.83681
6L8	-14943.99282	-4.813688	0.679	2.707	1.572	50.9	-3.85643
7L8	-17434.67332	-4.828298	0.680	2.713	1.578	51.0	-3.87115
8L8	-19925.35348	-4.838956	0.680	2.712	1.582	51.1	-3.88096
9L8	-22416.03351	-4.847159	0.680	2.714	1.585	51.1	-3.88832

^a MC(wa) values are given to 3 decimal places. Refer to Table 1 reference 11 for more significant figs. ^b See footnote b for Table 1 ^c See equation {3} and discussion below.

We now consider these data. First it is important to note that within each family, the nanotubes become more stable with increased length, as indicated by the increase in cohesive energy. Tracing the origin of this trend demands new protocols, which are now developed using the relationship between cohesive (E_{coh}) and coulombic energies (E_{coul} in Tables 1-3). In general this can be framed as follows:

$$E_{\text{coul}} = (\text{MC}(\text{wa})) \cdot (z^+ \cdot z^-) / r \quad \{3\}$$

E_{coul} and E_{coh} are related by¹¹:

$$E_{\text{coul}} = E_{\text{coh}} + E \quad \{4\}$$

E contains principally repulsive terms which are independent of the Madelung Constant, as shown by the Born-Mayer relationship³:

$$E(\text{lattice energy}) = (\text{MC}(wa) \cdot (z^+ \cdot z^-)/r) + be^{-ar} \quad \{5\}$$

b is a compressibility constant and a is a constant associated with electronic repulsions.

The data presented in Tables 1-3 indicate that the average apparent partial ionic charges range from 0.65 to 0.73 a.u. This is an interesting property of the nanotubes suggesting that a significant part of the bonding interactions are not furnished by point charge monopole-monopole contributions. This has been discussed in depth by Madden and Wilson⁵ (see Introduction) and also by Stone¹⁵. In essence this is a consequence of polarization of anions leading to additional interactions throughout the lattice. Stone¹⁵, and Madden and Wilson⁵ have framed this in terms of the large anionic polarizabilities. In the case of NaCl, the polarizability of Na⁺ (about 1 a.u) is negligible to that of Cl⁻ (about 20 a.u)¹⁶. In the case where the anions are in different environments¹⁵ there are significant induction potentials arising from induced dipoles dictated by polarization of anions by unsymmetrically disposed cations. In the case of the NaCl nanotubes, the anions in each layer are in different environments. This is indeed reflected by the different MC values and ACN's (see Fig 1). Unlike in a bulk crystal, these effects are significant. For example, in the nanotube shown in Figure 1 which contains 42 ions (7 layers) each layer of anions is in a different environment with respect to the central layer (MC =1.615). We now report the relative ionic character for each family of nanotubes using the data assembled in Table 5. Rather than merely use the ionic charge as a measure of ionicity (i.e., by comparison with the bulk values, assumed to be +1 and -1) we also consider the $E_{\text{coul}}/E_{\text{coh}}$ ratio which we define as the nanotube ionicity. In each family of nanotubes, the percent ionicity ($100 \times E_{\text{coul}}/E_{\text{coh}}$) increases as the tubes lengthen. (see Tables 1-3). For example, for the L4 family the

ionicity increases from 53% (2L4) to 58% (10L4). The percent ionicity however decreases as the tubes widen which is in concert with the apparent ionic charges, but is intuitively surprising.

We now compare the changes in coulomb (electrostatic) energies and cohesive (total bonding energies) as the nanotubes grow in length using the data from Tables 1-3 (E_{coh} and E_{coul} columns). S and L designations below refer to the energies associated with shorter (S) and longer (L) tubes in a pairwise comparison.

$$E_{(\text{coul}L)} = E_{\text{coh}L} + E(L)$$

$$E_{(\text{coul}S)} = E_{\text{coh}S} + E(S)$$

$$\Delta E = E_{\text{coul}L} - E_{\text{coul}S} = E_{\text{coh}L} - E_{\text{coh}S} + (E(L) - E(S))$$

$$\Delta E_{\text{coul}} = \Delta E_{\text{coh}} + (E(L) - E(S)) \quad \{6\}$$

The convention adopted here is that ΔE is the energy of the longer tube minus that of the shorter. In addition, it follows importantly that if $\Delta E_{\text{coul}} = \Delta E_{\text{coh}}$ then changes in non-ionic (and repulsive) terms are negligible. This enables a direct assessment of the stabilization energies of the nanotubes with length, and is applicable to any alkali halide nanotube.

In the following paragraphs we present analyses based on equation {6} (the change in electrostatic versus cohesive energy) for L4, L6 and L8 NaCl nanotubes families. A comparison between the changes in the ionic energies (equation {6}) and cohesive energies (equation {2}) for adjacent tubes (e.g., the difference between 2L6 and 3L6) are given in Table 4).

Table 4. Differences in coulomb and cohesive energies (see equations {2} and {6}). Column 1 indicates the change in energies for specific tubes. (2-3 indicates that for L2 and L3 nanotubes). Energies are in atomic units. Blank entries indicate that DFT calculations were not performed due to computational time constraints.

	L4	L4	L6	L6	L8	L8
	ΔE_{coul}	ΔE_{coh}	ΔE_{coul}	ΔE_{coh}	ΔE_{coul}	ΔE_{coh}
1-2	-0.0168	-0.0170	-0.0129	-0.0129	-0.1170	-0.01167
2-3	-4.661×10^{-3}	-4.533×10^{-3}	-3.817×10^{-3}	-3.754×10^{-3}	-3.605×10^{-3}	-3.416×10^{-3}
3-4	-2.454×10^{-3}	-2.444×10^{-3}	-1.977×10^{-3}	-2.007×10^{-3}	-1.791×10^{-3}	-1.903×10^{-3}
4-5	-1.446×10^{-3}	-1.425×10^{-3}	-1.137×10^{-3}	-1.203×10^{-3}	-1.068×10^{-3}	-1.097×10^{-3}
5-6	-9.717×10^{-4}	-9.663×10^{-4}	-7.773×10^{-4}	-7.989×10^{-4}	-7.203×10^{-4}	-7.285×10^{-4}
6-7	-6.916×10^{-4}	-7.537×10^{-4}	-5.549×10^{-4}	-5.673×10^{-4}	-5.107×10^{-4}	-5.369×10^{-4}
7-8	-5.195×10^{-4}	-5.181×10^{-4}	-4.163×10^{-4}	-4.264×10^{-4}	---	---
8-9	-4.036×10^{-4}	-4.024×10^{-4}	-3.238×10^{-4}	-3.196×10^{-4}	---	---
9-10	-3.233×10^{-4}	-3.223×10^{-4}	---	---	---	---

These data present an opportunity to trace the source of the increased cohesive energy in a family of lengthening nanotubes. In all cases there is a good match between the change in coulomb energy (ΔE_{coul}), a purely electrostatic contribution, and the overall change in the cohesive energy (ΔE_{coh}) which contains both ionic and other interaction terms. The change in electrostatic and cohesive energies is essentially equal for all nanotubes. Thus the increasing stabilization with length must be almost completely electrostatic in origin. This new formalism therefore enables one to weigh ionic versus other contributions to the stabilization energies. Note that this approach is only possible via the computation of MC(wa) and recognition of the linear correlation between E_{coh} and MC(wa)¹¹ as shown in Fig 3.

This method (vide supra) can also be used to examine the bonding occurring in NaCl nanotubes with different diameters containing equal numbers of ions. As an example we use 3L8, 4L6 and 6L4 which are all composed of 24 ions. Data are assembled in Table 5.

Table 5. Data for NaCl nanotubes composed of 24 ions.

	3L8	4L6	6L4
$E_{\text{coul}}/\text{au}$	-0.1382	-0.1443	-0.1598
E_{coh}/au	-0.1732	-0.1743	
MC(wa)	1.5324	1.5457	1.5484
z/au	0.6768	0.6903	0.7280
$r/\text{\AA}$	2.684	2.697	2.714
$\Delta E_{\text{coul}}/\text{au}$	-6.12×10^{-3}	-0.0155	-----
$\Delta E_{\text{coh}}/\text{au}$	-0.0155	$+ 5.2 \times 10^{-4}$	-----
$E_{\text{coh}} \text{ v MC(wa) slope}/\text{au}^a$	-0.090	-0.093	-0.103
$E_{\text{coh}} \text{ v MC(wa) intercept}/\text{au}^a$	-0.0349	-0.0298	-0.138
$\Delta \text{ Intercept}/\text{au}$	0.0051	0.016	

^a Slope and Intercept are from Figure 2.

From Table 5 we can determine the difference between the changes in electrostatic energy (ΔE_{coul}) and the change in overall cohesive energy (ΔE_{coh}). Comparing the 3L8 and 4L6 nanotubes, the difference is $-6.12 \times 10^{-3} - (-1.15 \times 10^{-3}) = 0.005 \text{ a.u.}$ which matches the graphical Δ intercept ($-0.0298 - (-0.0349) = 0.0051$) for the $E_{\text{coh}} \text{ v MC(wa)}$ plot. For 4L6 to 6L4 the difference in energies is $(-0.0155 - 5.2 \times 10^{-4} = 0.016 \text{ au.})$, which also exactly matches change in intercept (see Table) 5. This is entirely consistent with equation {6} above. The last two terms (EL-ES) are the intercepts of the $E_{\text{coh}} \text{ v MC(wa)}$ plots (see Table 5). These data further consolidate the relationship between E_{coh} and MC(wa) (see Figure 3). The slopes provide the

charge on the ions, and the intercepts reflect changes in the repulsive energies. It is interesting to also note at this point, the linear $E_{\text{coh}} \text{ v } MC(\text{wa})$ plots demand that $z^+ \cdot z^- / r$ (the slope) must be a constant for each family of nanotubes. As z increases then r must decrease which is intuitively satisfying but the perfect linear relationship is remarkable.

A new linear relationship is now introduced that links $MC(\text{wa})$ and the average coordination number (ACN) of the ions in each nanotube. This is illustrated in Figure 4. Mathematically this means that the finite sum used to compute $MC(\text{wa})$ for a family of nanotubes is factorable via the ACN. Physically however this has far-reaching implications. The linear correlation between ACN and MC is remarkable. It indicates that ACN's can replace $MC(\text{wa})$ in these analyses. ACN's are easily calculated using the formula presented above (see Computational Methods), while $MC(\text{wa})$ determinations require lattice sums to be evaluated which can be difficult for more complex structures such as spinels and perovskites.

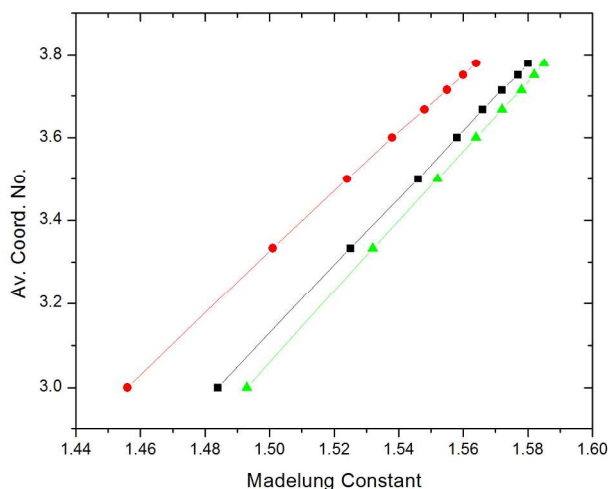


Figure 4. Linear correlation between ACN and $MC(\text{wa})$. Top to bottom, 4L, 6L, 8L.

SUMMARY AND CONCLUSIONS

In this paper, a new formalism has been developed to probe bonding contributions in NaCl nanotubes. This was built upon the key linear correlation between the weighted-average Madelung Constant and the cohesive energy.

New insights that have evolved from this work are:

- For small nanotubes, the ionic bonding contribution is significantly smaller than for a bulk crystal. This is furnished via the polarizations in different environments
- Increased stability of NaCl nanotubes with length is afforded mainly by ionic interactions.
- The average partial charges on the nanotube ions can be determined via a perfect linear relationship between the cohesive energies and weighted-average Madelung Constants.
- The percent ionicity of the nanotubes is revealed by a comparison of coulomb and cohesive energies.
- $z^+ \cdot z^- / r$ is a constant for NaCl nanotubes formed from layers of essentially regular polygons.
- There is a linear relationship between the average coordination number of the ions in any nanotube and the weighted-average Madelung Constant.
- Decreasing widths of the tubes favor higher ionic character.

FUTURE WORK

An interesting conclusion of this work points to fractional ionic charges, substantially smaller than for bulk NaCl. It will interesting is to compare the derived charges for the optimized

structures with those obtained using other theoretical approaches such as the Geodesic scheme developed by Spackman¹⁷ and Atomic Polar Tensor Analyses outlined by Chen et al.¹⁴ The fractional charges reflect a diminished charge transfer (CT) between the nanotube ions, and the methodology proposed here could serve as a probe of CT in more complicated systems, such as organic salts.⁹ In addition, studies will be performed using different basis sets with the addition of diffuse functions which should improve the DFT energies for these partially ionic nanostructures.

ACKNOWLEDGEMENTS

ADB acknowledges the receipt of PSC-CUNY grants 69597-0038 and 65790-0043 which supported this research. CRHH gratefully acknowledges support from PSC-CUNY grant TRADA-44-168. We thank Dr. Uwe Oehler (University of Guelph) for his immense patience and help designing programs used in this work. We thank the reviewers for very useful suggestions.

REFERENCES

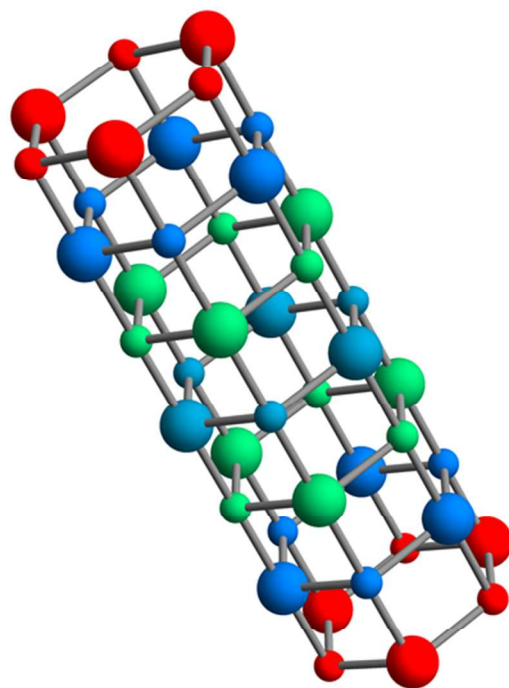
1. Welch,D.O.; Lazareth,O.W.; Dienes,G.J.; Hatcher,R.D. Clusters of Alkali Halide Molecules. *J. Chem. Phys.* **1997**, *68*, 2159-2171
2. Martin,T.P. Alkali Halide Clusters and Microcrystals. *Physics Reports* **1983**, *95*, 167-199
3. deKock,R.L.; Gray,H. “*Chemical Structure and Bonding*”. University Science Books; 2nd Ed. (1989) p457

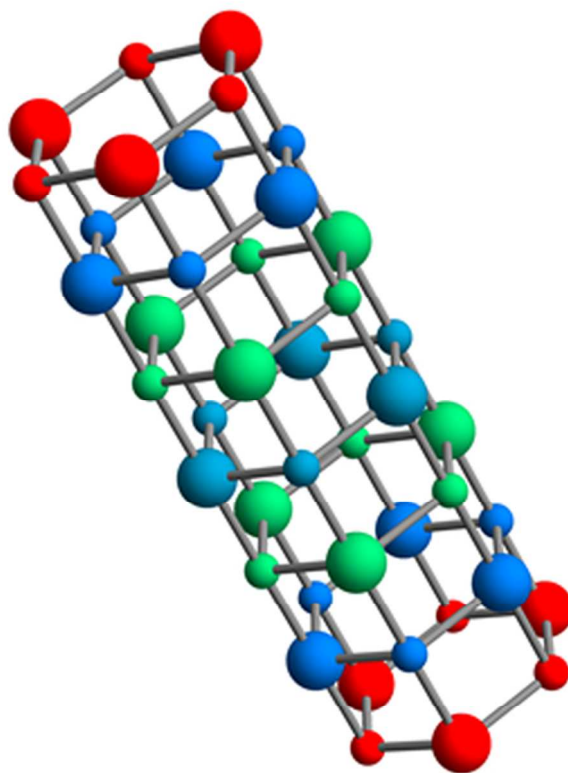
- 0
1
2
3
4
5
6
7
8
9
0
1
2
3
4
5
6
7
8
9
0
1
2
3
4
5
6
7
8
9
0
1
2
3
4
5
6
7
8
9
0
1
2
3
4
5
6
7
8
9
0
4. Salanne,M.; Madden,P.A. Polarization Effects in Ionic Solids and Melts. *Mol. Phys.* **2011**, *109*, 2299-2315
 5. Madden,P.A. ; Wilson,M. Covalent Effects in Ionic Systems. *Chem. Soc. Reviews*, **1996**, *25*, 339-350
 6. Kabrede,H.; Hentschke,R. An Improved Genetic Algorithm for Global Optimization and Its Application to Sodium Chloride Clusters. *J. Phys. Chem. B* **2002**, *106*, 10089-10095
 7. Fernandez-Lima,F.A.; Henkes,V. H.; da Silveira,E.F.; Nascimento,M.A.C. Alkali Halide Nanotubes: Structure and Stability. *J. Phys. Chem. C* **2012**, *116*, 4965-4969
 8. Baker,A.D.; Baker,M.D. Madelung Constants of Nanoparticles and Nanosurfaces. *J. Phys. Chem. C* **2009**, *113*, 14793-14797
 9. Izgorodina,E.I.;Bernard,U.L.;Dean,P.M.; Pringle,J.M.; MacFarlane,D.R. The Madelung Constant of Organic Salts. *Cryst. Growth and Design*. **2009**, *9*, 4834-4839
 10. Maroulis,G. Evaluating the Performance of DFT Methods in Electric Property Calculations: Sodium Chloride as a Test Case. *Rep. Theor. Chem.* **2013**, *2*, 1-8
 11. Baker,M.D.; Baker,A .D.; Belanger,J.; Hanusa,C.R.H.; Michaels,A. Linear Relationship Between Weighted-Average Madelung Constants and Density Functional Theory Energies for MgO Nanotubes. *J. Phys. Chem. C.* **2012**, *116*, 25588-25593
 12. Baker,A.D.; Baker,M.D. Rapid Calculation of Individual Ion Madelung Constants and their Convergence to Bulk Values. *Am. J. Phys.* **2010** ,*78*, 102-105

13. Gaussian 09. Revision A.02, Frisch,M.J.; Trucks,G.W.; Schlegel,H.B.; Scuseria,G.E.; Robb,M.A.; Cheeseman,J.R.; Scalmani,G.; Barone,V.; Mennucci,B.; Petersson,G.A.; et al.
14. Chen,L.; Xu,C.; Zhang,X.; Cheng,C.; Zhou,T. Size Dependent Structural and Electronic Properties of MgO Nanotube Clusters. *Int. J. Quant. Chem.* **2009**, *108*, 349-356
15. Stone, A. “*The Theory of Intermolecular Forces*”. Oxford University Press; 2nd Ed. (2013) Chapter 10.
16. Fowler, P.W.; Madden,P.A. In-crystal Polarizabilities of Alkali and Halide Ions. *Phys. Rev. B* **1984**, *29*, 1035-1042
17. Spackman,M.A. Potential Derived Charges Using a Geodesic Point Charge Selection Scheme. *J. Comp. Chem.* **1996**,*17*,1-18

0
1
2
3
4
5
6
7
8
9
0
1
2
3
4
5
6
7
8
9
0
1
2
3
4
5
6
7
8
9
0
1
2
3
4
5
6
7
8
9
0

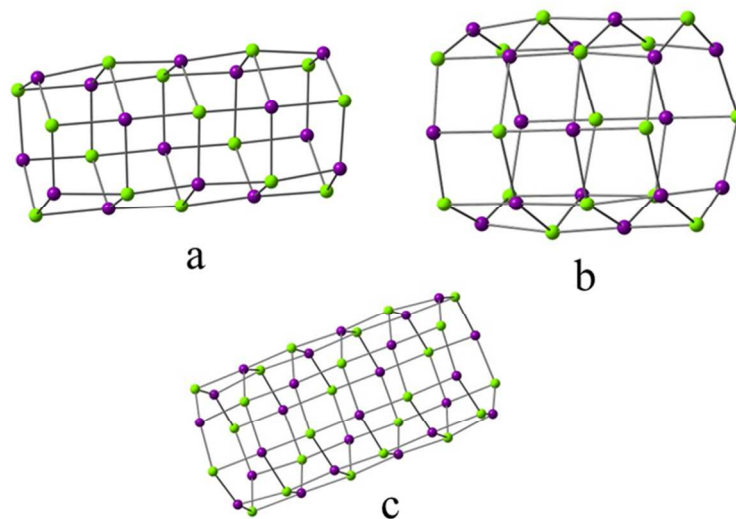
TOC GRAPHIC.

Madelung Map0
1
2
3
4
5
6
7
8
9
0
1
2
3
4
5
6
7
8
9
0
1
2
3
4
5
6
7
8
9
0
1
2
3
4
5
6
7
8
9
0



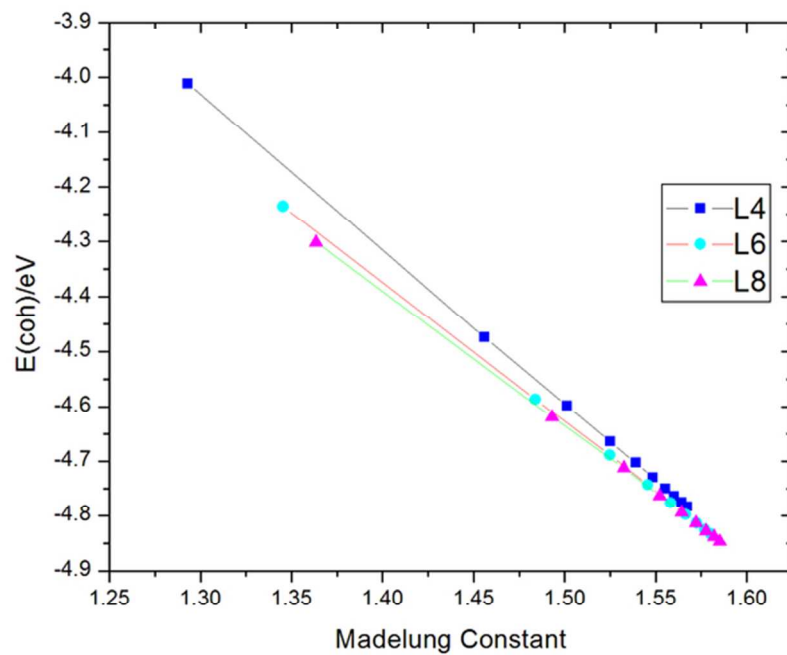
Madelung Constants for a 7L6 NaCl nanotube: Note that anions and cations in each layer have the same values. $MC(wa)$ is determined from the population distributions of the individual Madelung Constants. For this nanotube $MC(wa) = 1.572$ (see also Table 2). The least stable ions are situated at tube ends ($MC = 1.477$) and the most stable are located in the central layer ($MC = 1.615$).

75x69mm (300 x 300 DPI)

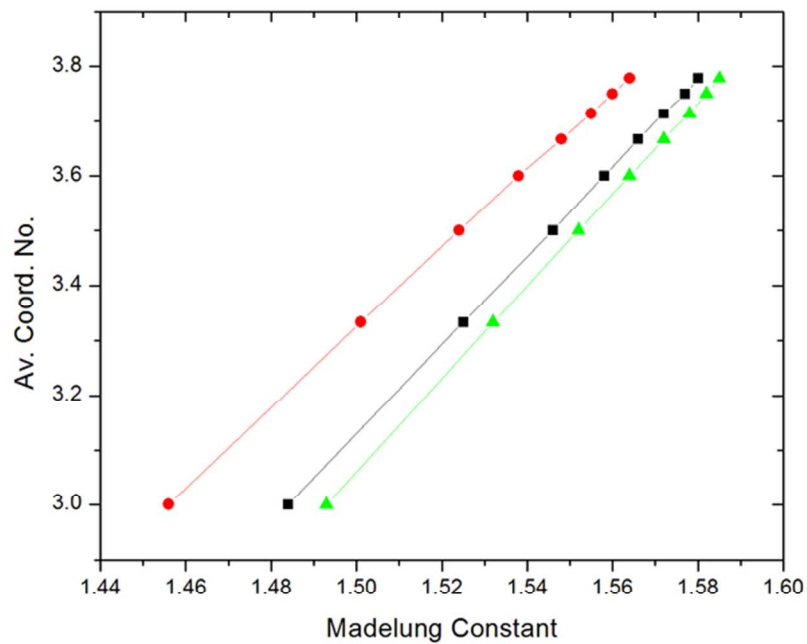


Madelung Constants for a 7L6 NaCl nanotube: Note that anions and cations in each layer have the same values. $MC(wa)$ is determined from the population distributions of the individual Madelung Constants. For this nanotube $MC(wa) = 1.572$ (see also Table 2). The least stable ions are situated at tube ends ($MC = 1.477$) and the most stable are located in the central layer ($MC = 1.615$).

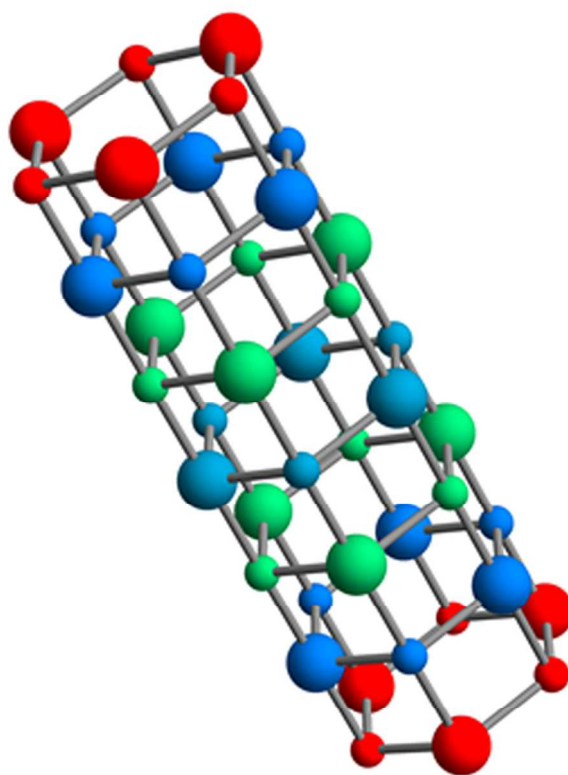
82x61mm (300 x 300 DPI)



Linear correlation between cohesive energies and weighted-average Madelung Constants for geometry (DFT) optimized L4, L6 and L8 NaCl nanotubes (top to bottom). In each case the correlation coefficient is 1.
63x48mm (300 x 300 DPI)



. Linear correlation between ACN and MC(wa). Top to bottom, 4L, 6L, 8L.
63x48mm (300 x 300 DPI)



Madelung Map
46x42mm (600 x 600 DPI)